Int. J. Heat Mass Transfer. Vol. 22, pp. 185–196

0017-9310/79/0201-0177 $02.00/0

WAVE INSTABILITY OF MIXED CONVECTION FLOW OVER A HORIZONTAL FLAT PLATE

T. S. CHEN and A. MUCOGLU*
Department of Mechanical and Aerospace Engineering,
University of Missouri-Rolla, Rolla, MO 65401, U.S.A.

(*Received* 23 *December* 1977 *and in revised form* 20 *June* 1978)

Abstract—The linear wave instability of laminar mixed convective flow over an isothermal horizontal flat plate is studied analytically. The main flow and thermal fields employed in the stability analysis are treated as non-parallel. The system of linearized, coupled differential equations and their boundary conditions for the velocity and temperature disturbances constitutes an eigenvalue problem that is solved by a direct Runge–Kutta numerical integration scheme along with an iteration procedure. A filtering technique is employed to remove the truncation errors inherent in the numerical integration of the disturbance equations. Neutral stability curves and critical Reynolds numbers are presented for a range of values of buoyancy parameter covering both assisting and opposing flow situations for Prandtl numbers of 0.7 and 7.0. In general, it is found that the flow becomes less stable as the buoyancy force increases for the opposing flow. The regions of stable and unstable flows are also mapped out in a Grashof number vs Reynolds number plane. Finally, the present results from wave instability are compared with those from vortex instability.

NOMENCLATURE

c, dimensionless phase velocity;
c_r, real part of c;
c_i, imaginary part of c;
c_p, specific heat at constant pressure;
D^n, differential operator, $d^n/d\eta^n$;
F, reduced stream function, equation (8);
G, ξ-derivative of F;
g, gravitational acceleration;
Gr_x, local Grashof number, $g\beta(T_w - T_\infty)x^3/\nu^2$;
Gr_L, Grashof number based on L, $g\beta(T_w - T_\infty)L^3/\nu^2$;
k, thermal conductivity;
L, characteristic length, $(\nu x/u_\infty)^{1/2}$;
p, mainflow pressure;
Pr, Prandtl number;
Re_x, local Reynolds number, $u_\infty x/\nu$;
Re_L, Reynolds number based on L, $u_\infty L/\nu$;
s, dimensionless temperature disturbance amplitude function;
T, mainflow temperature;
T_w, wall temperature;
T_∞, free stream temperature;
t, time;
U, dimensionless mainflow axial velocity component;
u, mainflow axial velocity component;
u_∞, free stream velocity;
V, dimensionless mainflow normal velocity component;
v, mainflow normal velocity component;
x, axial coordinate;
y, normal coordinate.

Greek symbols

α, dimensionless wavenumber based on L;
β, coefficient of thermal expansion;
η, pseudo-similarity variable, equation (6);
η_∞, dimensionless boundary-layer thickness;
θ, dimensionless temperature, equation (8);
ν, kinematic viscosity;
ξ, buoyancy parameter, $|Gr_x|/Re_x^{5/2}$;
ρ, density;
Φ, ξ-derivative of θ;
ϕ, dimensionless velocity disturbance amplitude function;
ψ, stream function of mainflow.

Superscripts

$'$ perturbation quantity;
$\hat{}$ total quantity (mainflow quantity plus perturbation quantity).

INTRODUCTION

IN MANY transport processes involving forced convection, the flow may be modified considerably by buoyancy forces due to temperature variations in the fluid. As a result of the buoyancy force effects, the flow regime may be affected such that the forced flow becomes unstable and the transport characteristics change. It is, therefore, of great importance to analyze the stability characteristics of laminar mixed forced and free convection flow. There are two modes of instability, the Tollmien–Schlichting wave instability and the thermal or vortex instability, which commonly arise in laminar flow over a horizontal or inclined surface in the presence of temperature variations in the fluid.

* Present address: Department of Mechanical Engineering, Villanova University, Villanova, PA 19085, U.S.A.

The linear stability of the plane-wave mode of disturbances (i.e. the Tollmien–Schlichting waves) for Blasius flow has been studied extensively under both parallel and nonparallel main flow assumptions. It has been shown [1] that for forced convection the nonparallel flow model contributes to the destabilization of the main flow. In addition, in the absence of buoyancy force effect, it has been found that when the effect of viscosity variation with temperature is included, heating of the fluid has a stabilizing effect, whereas cooling has a destabilizing effect [2]. The linear wave instability of free convection flow over horizontal and inclined surfaces has been studied, but not as extensively as for the case of vertical flat plates. Gebhart [3] has made an excellent survey of analytical and experimental studies on this subject. It has been found that in such flow situations the coupling of temperature and velocity disturbances has a destabilizing effect. Recently, Haaland and Sparrow [4] investigated the plane-wave instability of free convection on inclined surfaces. They found that, as compared to the parallel flow model, treating the main flow as nonparallel shifts the neutral stability curves to higher Grashof numbers and higher wave numbers. They also found that as the angle of plate inclination relative to the horizontal is increased from 45 to 135°, i.e. from upward-facing (45–90°) to downward-facing (90–135°), the flow becomes more and more stabilized. This is in agreement with the experimental results of Lock *et al.* [5]. From a study of plane-wave instability of free convection boundary-layer flow over horizontal and slightly inclined surfaces, Pera and Gebhart [6] also concluded that inclination stabilizes the flow.

Recently, the thermal or vortex instability of horizontal, laminar forced convection boundary-layer flow has received some attention [7, 8]. In a study on the instability of longitudinal vortices in forced convection flow adjacent to a horizontal flat plate, i.e. the Blasius flow, Wu and Cheng [7] employed a nonparallel flow model and considered the streamwise variation of the main flow and temperature fields in their analysis. They obtained the critical values of $Gr_x/Re_x^{3/2}$ (in which Gr_x and Re_x are, respectively, the local Grashof number and the local Reynolds number) for Prandtl numbers ranging from 10^{-2} to 10^4 and found that as the Prandtl number increases the critical value of $Gr_x/Re_x^{3/2}$ decreases.

In an analysis of laminar mixed convection flow over horizontal flat plates, Chen *et al.* [9] showed that the buoyancy forces arising from density variations due to the temperature gradients in a fluid modify considerably its flow and thermal fields. It is, therefore, of great interest to examinine the effects of buoyancy force on the stability characteristics of such a mixed convection flow. This has motivated the present investigation.

The present study deals with linear plane-wave instability of laminar, mixed forced and free convection boundary-layer flow along an isothermal horizontal flat plate. In the analysis, the temporal mode of disturbances are considered, and the main flow and thermal fields are derived from the local nonsimilarity solution. The main feature of this solution for the main flow is that it provides accurate flow and thermal fields that are continuous functions of the coordinate system. The governing differential equations of the disturbances for the velocity and temperature fields, which are coupled through the buoyancy forces, are obtained by linearization in which the nonparallelism of the main flow and thermal fields are taken into account. The resulting eigenvalue problem is solved by a direct Runge–Kutta integration scheme along with an iteration procedure. To remove the "parasitic errors" inherent in the numerical integration of the disturbance equations, a filtering technique introduced by Kaplan [10] is employed after each step of integration. Neutral stability curves and critical Reynolds numbers are presented for a range of values of buoyancy parameter covering both assisting and opposing flows, for Prandtl numbers of 0.7 and 7. The stable and unstable flow regimes are distinguished in terms of critical Reynolds and Grashof numbers. Finally, the critical Reynolds numbers from the present analysis for plane-wave instability are compared with the analytical results of Wu and Cheng [7] and the experimental data of Gilpin *et al.* [11] from the standpoint of thermal instability.

ANALYSIS

The main flow and thermal fields

In analyzing the flow stability characteristics, one needs to know the velocity and temperature fields of the main flow. In the present analysis, the main flow quantities are derived from the work of Chen *et al.* [9], who employed a local nonsimilarity method to solve the transformed conservation equations of the laminar boundary layer. The system of differential equations describing the main flow as given by Chen *et al.* [9] for the local nonsimilarity model truncated at the second level are:

$$F'''' + \frac{1}{2}(FF''' + F'F'') \pm \frac{1}{2}\xi\eta\theta' \mp \frac{1}{2}\xi^2\Phi = \frac{1}{2}\xi(F'G'' - F'''G) \quad (1)$$

$$G'''' + \frac{1}{2}(FG''' + F''G') + F'''G \pm \frac{1}{2}\eta(\theta' + \xi\Phi') \mp \xi\Phi + \frac{1}{2}\xi(GG''' - G'G'') = 0 \quad (2)$$

$$\frac{1}{Pr}\theta'' + \frac{1}{2}F\theta' = \frac{1}{2}\xi(F'\Phi - \theta'G) \quad (3)$$

$$\frac{1}{Pr}\Phi'' + F\Phi' - \frac{1}{2}F'\Phi + G\theta' + \frac{1}{2}\xi(G\Phi' - G'\Phi) = 0 \quad (4)$$

with the boundary conditions

$$F'(\xi,0)=F(\xi,0)=G'(\xi,0)=G(\xi,0)=\Phi(\xi,0)=0,\quad \theta(\xi,0)=1 \tag{5a}$$

$$F''(\xi,0)=\mp\frac{1}{2}\xi\int_0^\infty\theta\,d\eta\mp\frac{1}{2}\xi^2\int_0^\infty\Phi\,d\eta \tag{5b}$$

$$G''(\xi,0)=\mp\frac{1}{2}\int_0^\infty\theta\,d\eta\mp\frac{3}{2}\xi\int_0^\infty\Phi\,d\eta \tag{5c}$$

$$F'(\xi,\infty)=1,\ G(\xi,\infty)=\theta(\xi,\infty)=\Phi(\xi,\infty)=0. \tag{5d}$$

In the foregoing equations, the buoyancy parameter $\xi(x)$ and the pseudosimilarity variable $\eta(x,y)$ are defined, respectively, as

$$\xi=\frac{|Gr_x|}{Re_x^{5/2}},\quad \eta=y\left(\frac{u_\infty}{\nu x}\right)^{1/2} \tag{6}$$

where x and y are the axial and normal coordinates, u_∞ is the free stream velocity, and the local Grashof number Gr_x and the local Reynolds number Re_x are defined, respectively, by

$$Gr_x=g\beta(T_w-T_\infty)x^3/\nu^2,\quad Re_x=u_\infty x/\nu. \tag{7}$$

The reduced stream function $F(\xi,\eta)$ and the dimensionless temperature $\theta(\xi,\eta)$ have the expressions

$$F(\xi,\eta)=\frac{\psi(x,y)}{(\nu u_\infty x)^{1/2}},\quad \theta(\xi,\eta)=\frac{T-T_\infty}{T_w-T_\infty} \tag{8}$$

where T_w is the wall temperature, T_∞ is the free stream temperature, and $\psi(x)$ is the stream function that satisfies the continuity equation with

$$u=\frac{\partial\psi}{\partial y},\quad v=-\frac{\partial\psi}{\partial x}. \tag{9}$$

The primes in equations (1)–(5) denote partial differentiation with respect to η and the dependent variables G and Φ are defined by

$$G=\frac{\partial F}{\partial\xi},\quad \Phi=\frac{\partial\theta}{\partial\xi}. \tag{10}$$

The upper sign in the dual signs $\pm$ or $\mp$ in front of some of the terms in equations (1), (2) and (5) apply to assisting flow (i.e. $T_w>T_\infty$ for flow above the plate and $T_w<T_\infty$ for flow below the plate) and the lower sign to opposing flow (i.e. $T_w<T_\infty$ and $T_w>T_\infty$, respectively, for flow above and below the plate). For flow below the plate, however, the temperature difference in the Gr_x expression needs to be replaced by $(T_\infty-T_w)$.

Formulation of the stability problem

Consider a two-dimensional flow over a horizontal flat plate with velocity components $\hat{u}$ and $\hat{v}$, respectively, in the streamwise and transverse directions (i.e. in the x and y coordinates), static pressure $\hat{p}$, and temperature $\hat{T}$. If the main flow quantities are u, v, p and T, upon which are superposed the perturbation quantities u', v', p' and T', one can write

$$\begin{aligned}\hat{u}&=u(x,y)+u'(x,y,t)\\ \hat{v}&=v(x,y)+v'(x,y,t)\\ \hat{p}&=p(x,y)+p'(x,y,t)\\ \hat{T}&=T(x,y)+T'(x,y,t).\end{aligned} \tag{11}$$

Since the main flow satisfies the conservation equations, substitution of equation (11) into Navier–Stokes equations and the energy equation for incompressible, two-dimensional time dependent fluid flow, followed by subtraction of the main flow and linearization of the disturbance quantities leads to the following disturbance equations:

$$\frac{\partial u'}{\partial t}+u\frac{\partial u'}{\partial x}+u'\frac{\partial u}{\partial x}+v\frac{\partial u'}{\partial y}+v'\frac{\partial u}{\partial y}=-\frac{1}{\rho}\frac{\partial p'}{\partial x}+\nu\left(\frac{\partial^2u'}{\partial x^2}+\frac{\partial^2u'}{\partial y^2}\right) \tag{12}$$

$$\frac{\partial v'}{\partial t}+u\frac{\partial v'}{\partial x}+u'\frac{\partial v}{\partial x}+v\frac{\partial v'}{\partial y}+v'\frac{\partial v}{\partial y}=-\frac{1}{\rho}\frac{\partial p'}{\partial y}+\nu\left(\frac{\partial^2v'}{\partial x^2}+\frac{\partial^2v'}{\partial y^2}\right)\pm g\beta T' \tag{13}$$

$$\frac{\partial T'}{\partial t}+u\frac{\partial T'}{\partial x}+u'\frac{\partial T}{\partial x}+v\frac{\partial T'}{\partial y}+v'\frac{\partial T}{\partial y}=\frac{k}{\rho c_p}\left(\frac{\partial^2T'}{\partial x^2}+\frac{\partial^2T'}{\partial y^2}\right). \tag{14}$$

The positive and negative signs in front of the buoyancy term in equation (13) refer, respectively, to flows above and below the plate.

The next step is to eliminate the pressure terms in equations (12) and (13) by cross-differentiation and subtraction. The resulting equation is further simplified by employing the continuity equation $\partial u/\partial x+\partial v/\partial y=0$ and the boundary-layer approximations

$$\frac{\partial^2u}{\partial x^2}\ll\frac{\partial^2u}{\partial y^2},\quad \frac{\partial^2v}{\partial x^2}\ll\frac{\partial^2v}{\partial y^2},\quad \frac{\partial^2T}{\partial x^2}\ll\frac{\partial^2T}{\partial y^2}. \tag{15}$$

With these operations, equations (12) and (13) can be combined to yield

$$\begin{aligned}&\frac{\partial^2u'}{\partial y\partial t}-\frac{\partial^2v'}{\partial x\partial t}+u\left(\frac{\partial^2u'}{\partial y\partial x}-\frac{\partial^2v'}{\partial x^2}\right)\\ &\quad+v\left(\frac{\partial^2u'}{\partial y^2}-\frac{\partial^2v'}{\partial y\partial x}\right)+v'\frac{\partial^2u}{\partial y^2}-u'\frac{\partial^2v}{\partial y^2}\\ &=\nu\left[\frac{\partial}{\partial y}\left(\frac{\partial^2u'}{\partial x^2}+\frac{\partial^2u'}{\partial y^2}\right)-\frac{\partial}{\partial x}\left(\frac{\partial^2v'}{\partial x^2}+\frac{\partial^2v'}{\partial y^2}\right)\right]\\ &\quad\mp g\beta\frac{\partial T'}{\partial x}.\end{aligned} \tag{16}$$

For the case in which the main flow and thermal fields are treated as parallel, [that is, $u=u(y)$, $v=0$, and $T=T(y)$], the two terms involving v and $\partial T/\partial x$ in equation (14) and the three terms involving v and $\partial^2v/\partial y^2$ in equation (16) vanish from these equations.

In the present study, the main interest is to investigate the effects of the non-parallelism of the main flow and thermal fields on the wave instability characteristics of the flow. Thus, the disturbances are assumed to have the form of a plane wave travelling in the streamwise direction x, with its amplitude function depending only on y. The perturbation velocities and temperature are then related to their respective disturbance amplitude functions ϕ' and s' through the expressions

$$\psi'(x, y, t) = \phi'(y)\, e^{i\alpha'(x - c't)} \tag{17}$$

$$T'(x, y, t) = s'(y)\, e^{i\alpha'(x - c't)} \tag{18}$$

where ψ' is the stream function of the flow disturbances which satisfies the continuity equation with

$$u' = \frac{\partial \psi'}{\partial y}, \quad v' = -\frac{\partial \psi'}{\partial x}. \tag{19}$$

For the temporal mode of disturbances, the wave number α' is a positive real number and the phase velocity $c' = c'_r + ic'_i$ is a complex number. The real part of c', c'_r, represents the phase velocity of wave propagation, while the imaginary part c'_i determines the attenuation or amplification of disturbances. The flow is stable, neutrally stable, or unstable depending on whether c'_i is negative, zero, or positive.

Substituting u', v' and T' from equations (17)–(19) into equations (16) and (14) results in

$$(u - c')\left(\frac{d^2\phi'}{dy^2} - \alpha'^2\phi'\right) - \frac{\partial^2 u}{\partial y^2}\phi' - \frac{i}{\alpha'}\left[v\left(\frac{d^3\phi'}{dy^3} - \alpha'^2\frac{d\phi'}{dy}\right) - \frac{\partial^2 v}{\partial y^2}\frac{d\phi'}{dy}\right] \pm g\beta s' = -i\frac{\nu}{\alpha'}\left[\frac{d^4\phi'}{dy^4} - 2\alpha'^2\frac{d^2\phi'}{dy^2} + \alpha^4\phi'\right] \tag{20}$$

$$(u - c')s' - \frac{i}{\alpha'}\frac{\partial T}{\partial x}\frac{d\phi'}{dy} - \frac{i}{\alpha'}v\frac{ds'}{dy} - \frac{\partial T}{\partial y}\phi' = -\frac{i}{\alpha'}\frac{k}{\rho c_p}\left(\frac{d^2 s'}{dy^2} - \alpha'^2 s'\right). \tag{21}$$

Next, equations (20) and (21) are non-dimensionalized by introducing the following dimensionless quantities

$$\eta = \frac{y}{L}, \quad U = \frac{u}{u_\infty}, \quad V = \frac{v}{u_\infty}, \quad s = \frac{s'}{T_w - T_\infty} \tag{22}$$

$$c = \frac{c'}{u_\infty}, \quad \alpha = \alpha' L, \quad \phi = \frac{\phi'}{u_\infty L}, \quad \theta = \frac{T - T_\infty}{T_w - T_\infty}$$

where the characteristic length L is defined by

$$L = \left(\frac{\nu x}{u_\infty}\right)^{1/2}. \tag{23}$$

The end result is

$$(U - c)(D^2 - \alpha^2)\phi - \frac{\partial^2 U}{\partial \eta^2}\phi - \frac{i}{\alpha}\left[V(D^3 - \alpha^2 D)\phi - \frac{\partial^2 V}{\partial \eta^2}D\phi\right] \pm \xi s = -\frac{i}{\alpha Re_L}(D^4 - 2\alpha^2 D^2 + \alpha^4)\phi \tag{24}$$

$$(U - c)s - \frac{i}{\alpha}VDs - \frac{\partial \theta}{\partial \eta}\phi - \frac{i}{\alpha Re_L}\left[\frac{1}{2}\left(\xi\frac{\partial \theta}{\partial \xi} - \eta\frac{\partial \theta}{\partial \eta}\right)\right]D\phi = -\frac{i}{\alpha Re_L Pr}(D^2 - \alpha^2)s \tag{25}$$

where $D^n = d^n/d\eta^n$, $\xi = |Gr_x|/Re_x^{5/2}$ is the buoyancy parameter as defined by equation (6) and $Re_L = u_\infty L/\nu$ is the Reynolds number based on the characteristic length L. The plus and minus signs in front of the buoyancy term in equation (24) apply for assisting and opposing flows, respectively. In arriving at equation (25), use is made of the relation

$$\frac{\partial T}{\partial x} = (T_w - T_\infty)\left(\frac{\partial \theta}{\partial \eta}\frac{\partial \eta}{\partial x} + \frac{\partial \theta}{\partial \xi}\frac{d\xi}{dx}\right). \tag{26}$$

The boundary conditions for equations (24) and (25) require that the disturbance velocities u', v', and temperature T' vanish at the plate surface and in the free stream outside the boundary layer. That is,

$$u' = v' = T' = 0 \quad at \quad y = 0 \tag{27a}$$

$$u' = v' = T' = 0 \quad as \quad y \to \infty. \tag{27b}$$

In terms of the amplitude functions ϕ and s these boundary conditions can be replaced with

$$\phi = D\phi = s = 0 \quad \text{at} \quad \eta = 0 \tag{28a}$$

$$\phi = D\phi = s \to 0 \quad \text{as} \quad \eta \to \infty. \tag{28b}$$

The main flow quantities U, V, θ and their derivatives appearing in equations (24) and (25) can be obtained from the solution of the main flow problem described by the system of equations (1)–(5). In particular, one can show that

$$U = \frac{\partial F}{\partial \eta}, \quad \frac{\partial^2 U}{\partial \eta^2} = \frac{\partial^3 F}{\partial \eta^3}$$

$$V = \frac{1}{2Re_L}\left(\eta\frac{\partial F}{\partial \eta} - F - \xi\frac{\partial F}{\partial \xi}\right)$$

$$\frac{\partial^2 V}{\partial \eta^2} = \frac{1}{2Re_L}\left(\frac{\partial^2 F}{\partial \eta^2} + \eta\frac{\partial^3 F}{\partial \eta^3} - \xi\frac{\partial^2 G}{\partial \eta^2}\right) \tag{29}$$

$$\frac{\partial \theta}{\partial \eta} = \theta', \quad \frac{\partial \theta}{\partial \xi} = \Phi.$$

The eigenvalue problem consisting of the coupled differential equations (24) and (25) along with the boundary conditions, equations (28), is of the form

$$E(Re_L, \alpha, c_r, c_i\ ;\ \xi, Pr) = 0. \tag{30}$$

The solution of equation (30) for given Pr and ξ

gives a relationship among α, Re_L, c_r, and c_i. In determining the neutral stability curves, the values of c_r and α or Re_L satisfying equation (30) are sought as the eigenvalues for given values of Re_L or α with $c_i = 0$.

NUMERICAL METHOD OF SOLUTION

The solutions to the main flow and thermal fields, as described by the system of equations (1)–(5) for the local nonsimilarity two-equation model, were carried out by a predictor–corrector integration scheme to improve the accuracy of the Runge–Kutta integration. A modified Newton–Raphson shooting method was employed to fulfil the conditions at the edge of the boundary layers. The details can be found in Chen *et al.* [9].

In solving the mathematical system for the stability problem, equations (24), (25) and (28), the Runge–Kutta integration scheme was used along with a filtering technique of Kaplan [10] to supress the growth of the parasitic errors inherent in the numerical integration. To start the integration, the boundary conditions as expressed by equations (28b) need to be replaced by appropriate conditions that are satisfied at a finite distance η_∞ from the plate, i.e. at the edge of the boundary layer. This can be achieved by obtaining the general solution of equations (24) and (25) evaluated at $\eta = \eta_\infty$. As shown in the Appendix, this gives rise to three sets of independent solutions (ϕ_1, s_1), (ϕ_2, s_2), and (ϕ_3, s_3) at $\eta = \eta_\infty$. For each set of the solutions, the integration of equations (24) and (25) starts at the edge of the boundary layer ($\eta = \eta_\infty$) and proceeds towards the wall ($\eta = 0$). For prescribed values of Pr and ξ, and with pre-assigned values of, say, Re_L and c_i or c_r and c_i, the eigenvalues α and c_r or Re_L and c_r are then determined by a differential correction shooting method until the boundary conditions for ϕ and s at the wall, equations (28a), are satisfied. The highlights of the numerical procedures are given in the Appendix.

In the numerical integration of the stability equations, a step size of $\Delta\eta = 0.04$ was found to be adequate for all the parameters ξ that were investigated. On the other hand, the step size for the integration of the main flow and thermal fields was taken as $\Delta\eta = 0.02$. In the numerical integrations of both the stability and main flow/thermal fields, the boundary layer thickness η_∞ ranged from 8 to 7 as the ξ parameter was varied from -0.02 to 0.10. All computations were performed on an IBM 370/165 digital computer using double precision arithmetic.

Table 1. Results for $F''(\xi,0)$ and $-\theta'(\xi,0)$, $Pr = 0.7$ and 7

$Pr = 0.7$			$Pr = 7$		
$Gr_x/Re_x^{5/2}$	$F''(\xi,0)$	$-\theta'(\xi,0)$	$Gr_x/Re_x^{5/2}$	$F''(\xi,0)$	$-\theta'(\xi,0)$
−0.0200	0.2961	0.2851			
−0.0150	0.3065	0.2874	−0.0075	0.3284	0.6442
−0.0100	0.3148	0.2895	−0.0050	0.3297	0.6449
−0.0010	0.33033	0.29232	−0.0010	0.33162	0.64584
−0.0005	0.33119	0.29251	−0.0005	0.33186	0.64596
0	0.33206	0.29268	0	0.33206	0.64591
0.0010	0.33377	0.29304	0.0010	0.33257	0.64634
0.0025	0.33633	0.29357	0.0025	0.33328	0.64671
0.0050	0.3406	0.2944	0.0050	0.3344	0.6472
0.0075	0.3448	0.2953	0.0075	0.3356	0.6478
0.01	0.3489	0.2961	0.01	0.3370	0.6484
0.02	0.3650	0.2993	0.02	0.3414	0.6508
0.03	0.3806	0.3023	0.03	0.3460	0.6531
0.04	0.3959	0.3051	0.04	0.3505	0.6554
0.05	0.4099	0.3077	0.05	0.3548	0.6576
0.06	0.4245	0.3104	0.06	0.3591	0.6598
0.07	0.4377	0.3126	0.07	0.3635	0.6619
0.08	0.4512	0.3148	0.08	0.3678	0.6641
0.09	0.4640	0.3171	0.09	0.3720	0.6661
0.10	0.4767	0.3193	0.10	0.3761	0.6682

RESULTS AND DISCUSSION

Numerical results were obtained for fluids with Prandtl numbers of 0.7 and 7 which are typical for air and water, respectively. The buoyancy force parameter $Gr_x/Re_x^{5/2}$ in the computations ranged from 0 to 0.1 for assisting flow ($Gr_x/Re_x^{5/2} > 0$) for both Prandtl numbers. For the opposing flow case ($Gr_x/Re_x^{5/2} < 0$), solutions were obtained for $Gr_x/Re_x^{5/2}$ values ranging from 0 to -0.02 for $Pr = 0.7$ and from 0 to -0.0075 for $Pr = 7$. The numerical results of $F''(\xi,0)$ and $-\theta'(\xi,0)$ from the solutions of the main flow and thermal fields are tabulated in Table 1.

Figures 1 and 2 show the neutral stability curves for representative buoyancy parameters, respectively for Prandtl numbers of 0.7 and 7. In the figures, the points along a neutral curve represent a neutrally stable flow ($c_i = 0$), the region inside the curve corresponds to an unstable flow ($c_i > 0$), and that outside the curve to a stable flow ($c_i < 0$). From Figs.

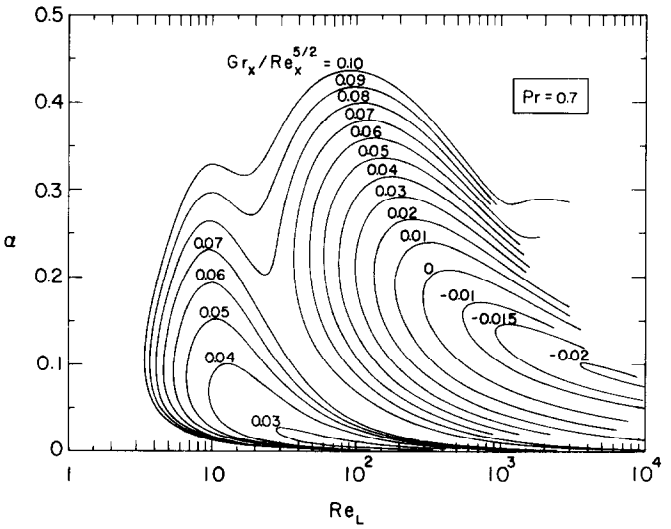

FIG. 1. Representative neutral stability curves, $Pr = 0.7$.

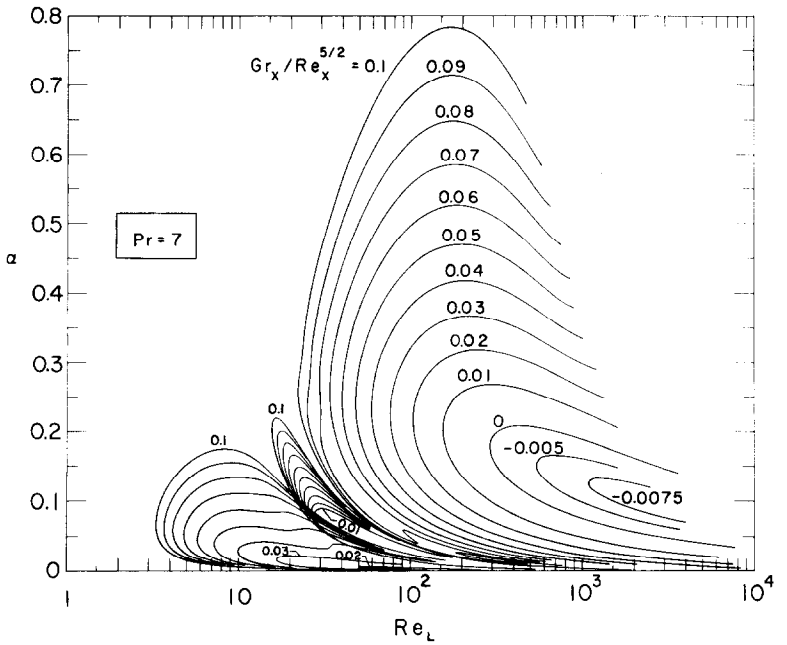

FIG. 2. Representative neutral stability curves, $Pr = 7$.

1 and 2, it can be seen that for assisting flow ($Gr_x/Re_x^{5/2} > 0$), the neutral stability curves for both $Pr = 0.7$ and 7 shift to a lower Reynolds number Re_L as the buoyancy parameter $Gr_x/Re_x^{5/2}$ increases; that is, the flow becomes less stable. This stability characteristic is believed to arise from the transfer of energy between the temperature and velocity disturbances in the forced flow. In the case of assisting flow, the buoyancy forces acting in the direction normal to the forced flow aid in moving the fluid particles away from the plate, and the interaction between the thermal and flow disturbances contributes to the destabilization of the forced flow. For the opposing flow, on the other hand, the flow becomes more stable as the buoyancy forces increase; that is the neutral stability curve shifts to a higher Reynolds number as $Gr_x/Re_x^{5/2}$ increases in the negative sense. In this case, the buoyancy forces aid in moving the fluid particles toward the plate and the interaction between thermal and flow disturbances enhances the stabilization of the forced flow. These behaviors of the neutral stability curves for assisting and opposing flow situations are similar to those obtained by Chen *et al.* [1, 12] for isothermal forced flow over horizontal plates with surface mass injection and suction, respectively.

An inspection of Figs. 1 and 2 reveals also that for assisting flow with certain buoyancy parameters, there exists more than one neutral stability curve for the same $Gr_x/Re_x^{5/2}$ value, each curve having a distinct range of phase speeds c_r and providing a different critical Reynolds number at a different

critical wavenumber. For example, for $Pr = 7$ and for a buoyancy parameter of $Gr_x/Re_x^{5/2} = 0.1$, one can see (Fig. 2) that there are three neutral stability curves. The three critical Reynolds numbers based on the characteristic length L, $Re_L^* = (u_\infty L/\nu)_{crit}$, are $Re_L^* = 3.3$, 15.6, and 22. The corresponding critical wavenumbers are $a^* = 0.065$, 0.205, and 0.26 (with critical wave velocities $c_r^* = 0.947$, 0.595, and 0.558), respectively. The maximum wavenumbers for the respective neutral curves are 0.175, 0.220, and 0.783. One can thus conclude that for $Gr_x/Re_x^{5/2} = 0.1$ and $Pr = 7$, all disturbances will decay when $Re_L < 3.3$, disturbances with wavenumbers larger than 0.175 will decay when $Re_L < 15.6$, and those with wavenumbers larger than 0.220 will die out when $Re_L < 22$. However, by considering the fact that disturbances in general travel with all possible wavenumbers, one will have to select the smallest of the critical Reynolds numbers, $Re_L^* = 3.3$, as the basis for the stability criterion in the above example. The existance of multiple neutral stability curves for the same buoyancy parameter will be explained later when the neutral stability curves from various flow models are compared in Figs. 6 and 7.

The critical Reynolds number Re_L^*, along with the corresponding critical wavenumbers α^* and critical wave velocities c_r^* for the $Gr_x/Re_x^{5/2}$ parameters that were investigated are listed in Tables 2 and 3, respectively for $Pr = 0.7$ and 7.

The critical Grashof numbers Gr_L^* (based on the characteristic length L) vs the critical Reynolds numbers Re_L^* are plotted in Figs. 3, 4 and 5. These results are computed from the critical Reynolds numbers Re_L^* at various buoyancy parameters $Gr_x/Re_x^{5/2}$. From the definition of Gr_L

$$Gr_L = g\beta(T_w - T_\infty)L^3/\nu^2 = Gr_x/Re_x^{3/2} \qquad (31)$$

and from equations (6), (7) and (23), one can arrive at the relationships

$$Re_x = Re_L^2, \quad Gr_x/Re_x^{5/2} = Gr_L/Re_L^2. \qquad (32)$$

Figures 3 and 4 show the Gr_L^* vs Re_L^* plots, respectively, for $Pr = 0.7$ and 7 for all the assisting flow parameters investigated and for the opposing flow cases with low buoyancy force parameters. The curves in Figs. 3 and 4 separate the stable flow region from the unstable one with regard to wave instabilities. Any flow condition as determined by any combination of the Reynolds number Re_L and Grashof number Gr_L, that lies above the curves

Table 2. Critical stability characteristics for $Pr = 0.7$

$Gr_x/Re_x^{5/2}$	α^*	Re_L^*	c_r^*
−0.0200	0.100	3515	0.224
−0.0150	0.137	925	0.309
−0.0100	0.156	551	0.349
−0.0010	0.176	305	0.399
−0.0005	0.177	297	0.401
0	0.177	290	0.403
0.0010	0.180	276	0.408
0.0025	0.183	257	0.414
0.0050	0.185	230	0.424
0.0075	0.188	207	0.435
0.01	0.190	188	0.443
0.02	0.203	132	0.481
0.03	0.210	99.0	0.514
	0.025	27.9	0.886
0.04	0.215	76.0	0.548
	0.070	9.5	0.928
0.05	0.220	59.8	0.583
	0.085	6.6	0.960
0.06	0.222	47.5	0.620
	0.090	5.4	0.944
0.07	0.223	37.2	0.663
	0.093	4.6	1.017
0.08	0.095	4.0	1.043
0.09	0.100	3.7	1.061
0.10	0.102	3.4	1.079

Table 3. Critical stability characteristics for $Pr = 7$

$Gr_x/Re_x^{5/2}$	α^*	Re_L^*	c_r^*	$Gr_x/Re_x^{5/2}$	α^*	Re_L^*	c_r^*
−0.0075	0.125	1066	0.316	0.04	0.235	59.2	0.489
−0.0050	0.150	539	0.362		0.105	24.0	0.507
−0.0010	0.175	318	0.397		0.030	9.9	0.785
−0.0005	0.176	303	0.401	0.05	0.240	47.9	0.501
0	0.177	290	0.403		0.120	22.5	0.530
0.0010	0.183	266	0.408		0.040	7.2	0.815
	0.070	28.8	0.420	0.06	0.245	39.8	0.513
0.0025	0.185	238	0.414		0.135	20.9	0.548
	0.070	28.7	0.421		0.045	5.7	0.850
0.0050	0.190	201	0.424	0.07	0.255	33.8	0.524
	0.071	28.5	0.425		0.152	19.4	0.564
0.0075	0.197	175	0.432		0.052	4.8	0.879
	0.074	28.0	0.432	0.08	0.275	29.3	0.534
0.01	0.200	155	0.438		0.170	18.0	0.577
	0.080	27.5	0.451		0.060	4.2	0.892
0.02	0.220	103	0.460	0.09	0.230	24.9	0.548
	0.085	26.5	0.464		0.185	16.7	0.585
	0.004	50.0	0.716		0.062	3.7	0.927
0.03	0.225	76.0	0.475	0.10	0.260	22.0	0.558
	0.095	25.3	0.488		0.205	15.6	0.595
	0.017	16.5	0.751		0.065	3.3	0.947

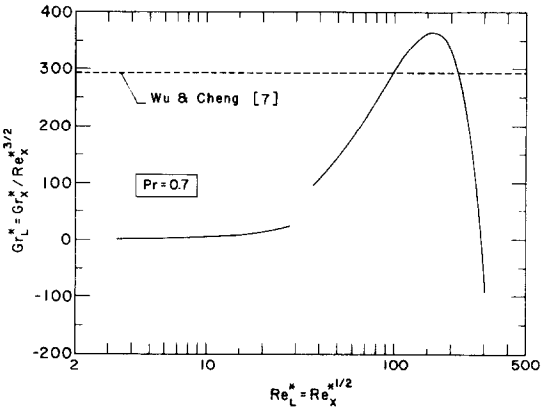

FIG. 3. Critical Grashof number vs critical Reynolds number, $Pr = 0.7$.

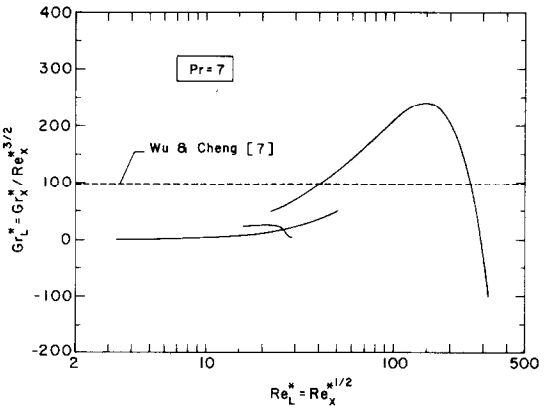

FIG. 4. Critical Grashof number vs critical Reynolds number, $Pr = 7$.

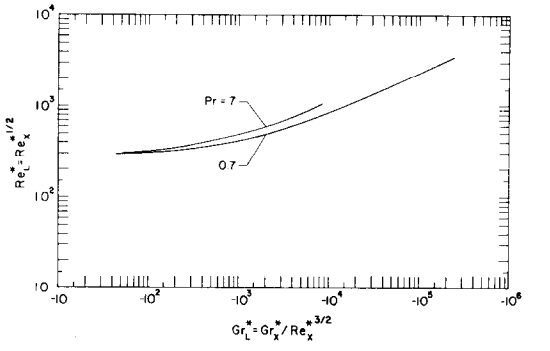

FIG. 5. Critical Reynolds number vs critical Grashof number for opposing flow, $Pr = 0.7$ and 7.

represents an unstable flow situation, while any point lying below the curves represents a stable one. For Prandtl number of 7, for example, a critical Grashof number of $Gr_L^* = 210$ (Fig. 4) gives a corresponding critical Reynolds number of $Re_L^* = 100$. From the relationships between Re_L and Re_x, equation (32), one finds that $Re_x^* = 10^4$. Thus, for a Reynolds number of $Re_L = 100$ or $Re_x = 10^4$ the flow will be stable to small disturbances when $Gr_L < 210$ or, from equation (32), $Gr_x < 2.1 \times 10^8$ and unstable when $Gr_L > 210$ or $Gr_x > 2.1 \times 10^8$. Similarly, when $Gr_L = 210$ (or $Gr_x = 2.1 \times 10^8$) the flow will be stable when $100 < Re_L < 193$ (or $10^4 < Re_x < 3.73 \times 10^4$) and unstable when $Re_L < 100$ or $Re_L > 193$. A comparison between Figs. 3 and 4 indicates that for assisting flow with Reynolds numbers $Re_L > 30$ (i.e. $Re_x > 900$), fluids with a Prandtl number of 0.7 are generally more stable to small disturbances than fluids with a Prandtl number of 7. However, the effect of the Prandtl numbers on the stability characteristics of the flow diminishes when $Re_x < 900$.

The results of Wu and Cheng [7] for the thermal (or vortex) instability of Blasius flow over a horizontal flat plate are also shown with dotted lines, respectively, in Figs. 3 and 4 for comparisons with the present wave instability results. The region below the dotted line represents flow conditions which are stable to vortex instabilities, while the region above pertains to flow conditions that are unstable to vortex instabilities. It can be seen from Fig. 3 for $Pr = 0.7$ that for Reynolds numbers $Re_L < 98$ and $Re_L > 218$ or $Re_x < 9.6 \times 10^3$ and $Re_x > 4.75 \times 10^4$, the flow is less susceptible to vortex disturbances. Thus, the first onset of instability is due to wave disturbances when $Re_x < 9.6 \times 10^3$ and $Re_x > 4.75 \times 10^4$. However, for $98 < Re_L < 218$ or $9.6 \times 10^3 < Re_x < 4.75 \times 10^4$, the instability of the flow is due to vortex disturbances. Similarly, for $Pr = 7$ (Fig. 4) one can see that the instability is initiated by wave disturbances when $Re_L < 40.7$ and $Re_L > 257$ or $Re_x < 1.65 \times 10^3$ and $Re_x > 6.6 \times 10^4$, whereas for $40.7 < Re_L < 257$ or $1.65 \times 10^3 < Re_x < 6.6 \times 10^4$ the instability of the flow is due to vortex disturbances.

The experimental study of Gilpin *et al.* [11] on the thermal instability of water flow over a heated horizontal flat plate with uniform surface temperature gives critical Grashof numbers Gr_L^* which range from 46 to 110, as compared to the analytical result of $Gr_L^* = 100$ for $Pr = 7$ given by Wu and Cheng [7] and shown in Fig. 4. The good agreement between the analytical and experimental results is unusual and surprising in view of the fact that linear theory normally predicts the onset of vortex instability at a Gr_L^* value that is lower in the order of magnitude than that observed in the experiments. In the work of Wu and Cheng [7], the effect of buoyancy force on the main flow was neglected in the analysis. In addition, it has been revealed that there were a couple of errors in the algebraic equations resulting from their formulation of the finite-difference form of the disturbance equations [13]. A preliminary study by the present authors has indicated that these two factors have contributed to the inaccuracy of the analytical results of Wu and Cheng [7]. The validity of their results is, therefore, open to questions and the comparisons of their results with the present wave instability results made in Figs. 3 and 4 should be regarded only as qualitative.

Figure 5 shows the Reynolds number vs Grashof number plot for the opposing flow case. In the figure, the region that lies above a curve is for unstable flow, while the region that lies below is for stable flow. In addition, it can be seen from the figure

that flow of fluids with a Prandtl number of 7 is more stable than flow of fluids with a Prandtl number of 0.7.

It is of interest to compare the neutral stability curves from the non-parallel flow model with those obtained from two approximate models: (a) the parallel flow model with temperature perturbations and (b) the non-parallel flow model without the temperature perturbations. For the parallel flow model, with the main flow and thermal fields being treated as parallel [i.e. $u = u(y)$, $v = 0$, $T = T(y)$], equations (24) and (25) for the velocity and temperature disturbances reduce to

$$(U-c)(D^2-\alpha^2)\phi-\left(\frac{\partial^2 U}{\partial \eta^2}\right)\phi \pm \xi s = -\frac{i}{\alpha Re_L}(D^4-2\alpha^2 D^2+\alpha^4)\phi \quad (33)$$

$$(U-c)s-\frac{\partial \theta}{\partial \eta}\phi = -\frac{i}{\alpha Re_L Pr}(D^2-\alpha^2)s. \quad (34)$$

In the non-parallel flow model without the temperature perturbations, the main flow is assumed to be non-parallel but the thermal field and the temperature disturbances are neglected altogether. Thus, the stability problem consists only of equation (24) without the buoyancy related ξs term, and equation (25) does not appear.

To compare typical neutral stability curves among the three flow models, Figs. 6 and 7 have been prepared, respectively, for $Pr = 0.7$ and 7. In each figure, curves are shown for representative buoyancy force parameters for assisting and opposing flows, along with the curve for pure forced convection ($Gr_x/Re_x^{5/2} = 0$). As can be seen from the figures, the parallel flow model provides critical Reynolds numbers that are somewhat higher than, but are generally in good agreement with, the nonparallel flow model. When the temperature disturbances are neglected in the nonparallel flow model, the stability of the flow is seen to increase and decrease tremendously for assisting flow ($Gr_x/Re_x^{5/2} > 0$) and opposing flow ($Gr_x/Re_x^{5/2} < 0$), respectively. The reason for this is that in the absence of the temperature disturbances, a favorable pressure gradient induced by the buoyancy force in the assisting flow case acts to aid the forced flow. As a result, the flow becomes more stable. For the opposing flow, on the other hand, the buoyancy force induces an adverse pressure gradient which retards the forced flow and thus contributes to the destabilization of the main flow.

It is interesting to observe from Figs. 6 and 7, along with Figs. 1 and 2, that multiple neutral stability curves exist only for assisting flow case at certain buoyancy force parameters under the condition of nonparallel flow model with temperature perturbations. These multiple neutral stability curves do not exist under the parallel flow model with temperature perturbations nor under the nonparallel flow model without the temperature perturbations.

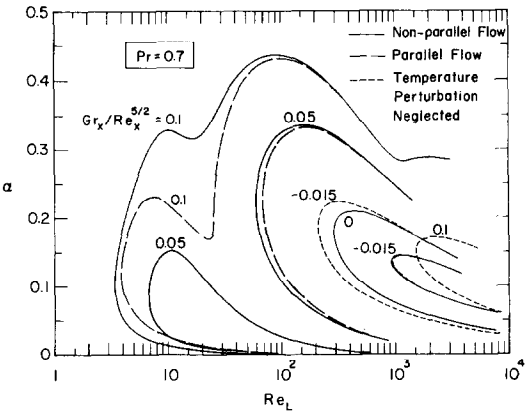

FIG. 6. A comparison of representative neutral stability curves among various models, $Pr = 0.7$.

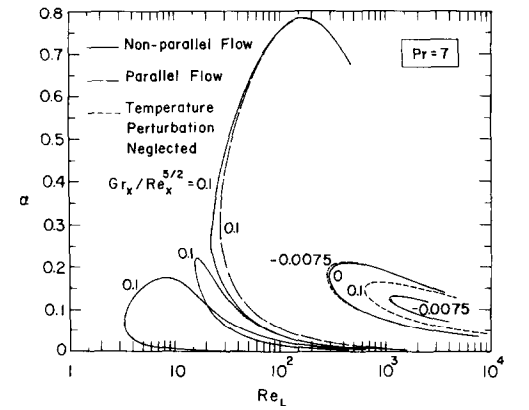

FIG. 7. A comparison of representative neutral stability curves among various models, $Pr = 7$.

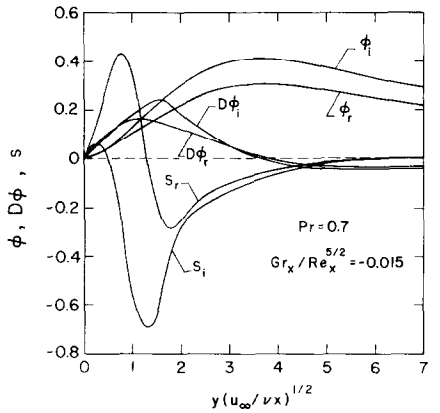

FIG. 8. Eigenfunctions for $\alpha = 0.137$, $Re_L = 925$, $c_r = 0.309$, and $c_i = 0$ with $Pr = 0.7$, $Gr_x/Re_x^{5/2} = -0.015$.

Thus, the nonparallelism of the main flow along with the existence of the temperature perturbations in assisting flow are responsible for the occurrence of the additional neutral stability curves. These two factors combined are then believed to induce a flow that is more unstable to a perturbed thermal wave than to a perturbed hydrodynamic wave, as evidenced by the existence of the extra neutral curves at a lower range of wavenumbers.

Representative eigenfunctions ϕ, $D\phi$ and s for $\alpha = 0.137$, $Re_L = 925$, $c_r = 0.309$ and $c_i = 0$ for the case of $Pr = 0.7$ and $Gr_x/Re_x^{5/2} = -0.015$ are shown in Fig. 8, where ϕ_r, $D\phi_r$, s_r denote the real parts and ϕ_i, $D\phi_i$, s_i the imaginary parts of the respective eigenfunctions.

CONCLUSIONS

An analysis has been performed to investigate the linear wave instability of laminar mixed convection flow over an isothermal horizontal flat plate. The eigenvalue problem consisting of the system of linearized, coupled differential equations for the disturbances along with their boundary conditions has been solved by a direct Runge–Kutta integration scheme, in conjunction with a filtering technique to remove the parasitic errors inherent in the numerical integration of the disturbance equations. Neutral stability curves and critical Reynolds numbers are presented for buoyancy parameter $Gr_x/Re_x^{5/2}$ ranging from -0.02 to 0.1 for a Prandtl number of 0.7 and from -0.0075 to 0.1 for a Prandtl number of 7. It is found that for assisting flow the flow becomes less stable to small disturbances as the buoyancy force increases, whereas for the opposing flow the flow becomes more stable as the buoyancy force increases. Multiple neutral stability curves are also found to exist in assisting flow over a certain range of the buoyancy force parameter. In addition, it is concluded that fluids with a Prandtl number of 0.7 are in general more stable to small disturbances than fluids with a Prandtl number of 7 for the case of assisting flow. The opposite trend is true for the opposing flow case.

Acknowledgements—This work was conducted under the auspices of NSF Grants ENG 75-15033 and ENG 75-15033 A01.

REFERENCES

1. T. S. Chen, E. M. Sparrow and F. K. Tsou, The effect of mainflow transverse velocities in linear stability theory, *J. Fluid Mech.* **50,** 741–750 (1971).
2. A. R. Wazzan, T. Okamura and A. M. O. Smith, The stability of water flow over heated and cooled flat plates, *J. Heat Transfer* **90,** 109–114 (1968).
3. B. Gebhart, Natural convection flow, instability, and transition, *J. Heat Transfer* **91,** 293–309 (1969).
4. S. E. Haaland and E. M. Sparrow, Wave instability of natural convection on inclined surfaces accounting for nonparallelism of the basic flow, *J. Heat Transfer* **96,** 405–407 (1973).
5. G. S. H. Lock, C. Gort and G. R. Pond, A study of instability in free convection from an inclined plate, *Appl. Scient. Res.* **18,** 171–182 (1967).
6. L. Pera and B. Gebhart, On the stability of natural convection boundary layer flow over horizontal and slightly inclined surfaces, *Int. J. Heat Mass Transfer* **16,** 1147–1163 (1973).
7. R. S. Wu and K. C. Cheng, Thermal instability of Blasius flow along horizontal plates, *Int. J. Heat Mass Transfer* **19,** 907–913 (1976).
8. K. C. Cheng and R. S. Wu, Maximum density effects on thermal instability of horizontal laminar boundary layers, *Appl. Scient. Res.* **31,** 465–479 (1976).
9. T. S. Chen, E. M. Sparrow and A. Mucoglu, Mixed convection in boundary layer flow on a horizontal plate, *J. Heat Transfer*, **99,** 66–71 (1977).
10. R. E. Kaplan, The stability of laminar incompressible boundary layer in the presence of compliant boundaries, ASRL, TR 116-1, MIT (1964).
11. R. R. Gilpin, H. Imura and K. C. Cheng, Experiments on the onset of longitudinal vortices in horizontal Blasius flow heated from below, *J. Heat Transfer* **100,** 71–77 (1978).
12. T. S. Chen and L. M. Huang, Hydrodynamic stability of boundary layers with surface suction, *AIAA Jl* **10,** 1366–1367 (1972).
13. K. C. Cheng, Private communication.

APPENDIX

Asymptotic solutions of ϕ and s and solution of the eigenvalue problem

At the edge of the boundary layer $\eta = \eta_\infty$, the mainflow quantities assume their asymptotic values and equations (24) and (25) reduce to

$$(1-c)(D^2-\alpha^2)\phi - \frac{i}{\alpha}V(\eta_\infty)(D^3-\alpha^2 D)\phi \pm \xi s = -\frac{i}{\alpha Re_L}(D^4-2\alpha^2 D^2+\alpha^4)\phi \quad \text{(A1)}$$

$$(1-c)s - \frac{i}{\alpha}V(\eta_\infty)Ds = -\frac{i}{\alpha Re_L Pr}(D^2-\alpha^2)s \quad \text{(A2)}$$

where

$$V(\eta_\infty) = \frac{1}{2Re_L}\left[\eta_\infty - F(\eta_\infty) - \xi\frac{\partial F(\eta_\infty)}{\partial \xi}\right]. \quad \text{(A3)}$$

From the linearity of the equations, the physically acceptable general solution to equations (A1) and (A2), after the elimination of the positively growing exponential solutions, assume the form

$$\phi(\eta_\infty) = c_1\phi_1(\eta_\infty) + c_2\phi_2(\eta_\infty) + c_3\phi_3(\eta_\infty) \quad \text{(A4a)}$$

$$s(\eta_\infty) = c_1 s_1(\eta_\infty) + c_2 s_2(\eta_\infty) + c_3 s_3(\eta_\infty) \quad \text{(A4b)}$$

where c_1, c_2 and c_3 are complex constants,

$$\phi_1(\eta_\infty) = \exp(-\alpha\eta_\infty), \quad \phi_2(\eta_\infty) = \frac{1}{m^2-\alpha^2}\exp(-m\eta_\infty),$$

$$\phi_3(\eta_\infty) = \frac{\pm i\alpha Re_L\xi}{(r^2-\alpha^2)[r^2-\alpha^2+rV(\eta_\infty)Re_L - i\alpha Re_L(1-c)]}\exp(-r\eta_\infty) \quad \text{(A5)}$$

$$s_1(\eta_\infty) = 0, \quad s_2(\eta_\infty) = 0, \quad s_3(\eta_\infty) = \exp(-r\eta_\infty)$$

and the exponents

$$m = -\frac{V(\eta_\infty)Re_L}{2} + \frac{1}{2}\{[V(\eta_\infty)Re_L]^2 + 4[\alpha^2 + i\alpha Re_L(1-c)]\}^{1/2}$$

$$r = -\frac{PrV(\eta_\infty)Re_L}{2} + \frac{1}{2}\{[PrV(\eta_\infty)Re_L]^2 + 4[\alpha^2 + i\alpha Re_L Pr(1-c)]\}^{1/2} \quad \text{(A6)}$$

are complex.

Equations (A4) provide three independent sets of solutions (ϕ_1, s_1), (ϕ_2, s_2), and (ϕ_3, s_3) at $\eta = \eta_\infty$. Thus, the complete solutions for ϕ and s at any η are given by

$$\phi(\eta) = c_1\phi_1(\eta)+c_2\phi_2(\eta)+c_3\phi_3(\eta) \tag{A7a}$$

$$s(\eta) = c_1 s_1(\eta)+c_2 s_2(\eta)+c_3 s_3(\eta) \tag{A7b}$$

where (ϕ_1, s_1), (ϕ_2, s_2), and (ϕ_3, s_3) satisfy equations (24), (25) and (28). A direct Runge–Kutta integration scheme was used to solve equations (24) and (25) for each of the three independent sets of solutions. At each step of the integration, the filtering technique of Kaplan [10] was applied to remove the parasitic errors that arise from truncation in the numerical integration so that the independence of each of the three sets of solutions for ϕ and s can be preserved.

The eigenvalue problem was solved in the following manner. With the values of Prandtl number Pr and buoyancy force parameter ξ prescribed, two of the four parameters α, Re_L, c_r, and c_i, say Re_L and c_i or α and c_i, are preassigned certain values, while the values of the two remaining parameters α and c_r or Re_L and c_r are guessed. The latter are the eigenvalues to be determined. Equations (24) and (25) are then integrated and the boundary conditions at the wall are checked to see if they are satisfied for the initially guessed eigenvalues. To do this, equations (A7) are evaluated at the wall ($\eta = 0$) for two of the three boundary conditions in equations (28a), $s(0) = D\phi(0) = 0$, along with a normalizing condition $D^2\phi = 1$ at $\eta = 0$:

$$\begin{aligned} s(0) &= 0 = c_1 s_1(0)+c_2 s_2(0)+c_3 s_3(0) \\ D\phi(0) &= 0 = c_1 D\phi_1(0)+c_2 D\phi_2(0)+c_3 D\phi_3(0) \\ D^2\phi(0) &= 1 = c_1 D^2\phi_1(0)+c_2 D^2\phi_2(0)+c_3 D^2\phi_3(0). \end{aligned} \tag{A8}$$

The complex constants c_1, c_2 and c_3 are determined from equations (A8), which are then substituted into the remaining boundary condition at the wall to see if

$$\phi(0) = 0 = c_1\phi_1(0)+c_2\phi_2(0)+c_3\phi_3(0) \tag{A9}$$

is satisfied. If the condition (A9) is not satisfied, the guessed eigenvalues are then improved by using a Newton–Raphson differential correction iteration scheme, until it is satisfied within a certain pre-assigned tolerance $|\varepsilon|$, say, $|\varepsilon| \leqslant 10^{-6}$.

INSTABILITE ONDULATOIRE D'UN ECOULEMENT DE CONVECTION MIXTE SUR UNE PLAQUE PLANE ET HORIZONTALE

Résumé—On étudie analytiquement l'instabilité linéaire d'un écoulement laminaire de convection mixte sur une plaque plane, horizontale et isotherme. Les champs d'écoulement principal et de température considérés dans cette analyse de stabilité sont traités comme n'étant pas parallèles. On résout par une méthode numérique d'intégration directe de Runge–Kutta, avec procédure d'itération, le système d'équations linéarisées et couplées, avec leurs conditions aux limites, pour les perturbations de vitesse et de température, système qui constitue un problème de valeurs propres. Une technique de filtrage est utilisée pour réduire les erreurs de troncature inhérantes à l'intégration numérique des équations de perturbation. Des courbes de stabilité neutre et des nombres de Reynolds critiques sont présentés pour un domaine de valeur du paramètre caractéristique couvrant aussi bien les situations d'écoulement favorisé que contrarié, pour des nombres de Prandtl de 0,7 et de 7. On trouve en général que lorsque la force d'Archimède augmente, l'écoulement favorisé devient moins stable alors que l'écoulement contrarié devient plus stable. Les régions d'écoulement stable ou instable sont représentées dans le plan nombre de Grashof, nombre de Reynolds. Ces résultats sur l'instabilité ondulatoire sont enfin comparés avec ceux de l'instabilité tourbillonnaire.

WELLENINSTABILITÄT DER STRÖMUNG BEI MISCHKONVEKTION AN EINER HORIZONTALEN EBENEN PLATTE

Zusammenfassung—Es wurde die lineare Welleninstabilität einer laminaren Strömung bei Mischkonvektion an einer isothermen horizontalen ebenen Platte analytisch untersucht. Die benutzten Hauptströmungs- und Temperaturfelder werden in der Stabilitätsanalyse als nichtparallel behandelt. Ein System von linearisierten, gekoppelten Differentialgleichungen und deren Randbedingungen für die Geschwindigkeits- und Temperaturstörungen stellt ein Eigenwertproblem dar. Dies wird mit Hilfe eines numerischen direkten Runge–Kutta-Integrationsschemas und eines Iterationsverfahrens gelöst. Es wurde eine Filterungstechnik benutzt, um die Rundungsfehler zu beseitigen, die untrennbar mit der numerischen Integration der Störungsgleichungen verbunden sind. Neutrale Stabilitätslinien und kritische Reynolds–Zahlen werden für eine Reihe von Werten der Auftriebsparameter angegeben, die sowohl gleichgerichtete als auch entgegengesetzte Strömungssituationen bei Prandtl–Zahlen von 0,7 bis 7,0 berücksichtigen. Im allgemeinen wurde festgestellt, daß die Strömung weniger stabil wird, wenn die Auftriebskraft bei gleichgerichteter Strömung zunimmt und daß sie bei entgegengerichteter Strömung mit Zunahme der Afutriebskraft stabiler wird. Gebiete der stabilen und instabilen Strömung sind in der Auftragung der Grashof–Zahl über der Reynolds–Zahl gekennzeichnet. Schließlich werden die vorliegenden Ergebnisse der Wellen instabilität mit denen der Wirbelinstabilität verglichen.

ВОЛНОВАЯ НЕУСТОЙЧИВОСТЬ ПОТОКА СМЕШАННОЙ КОНВЕКЦИИ НАД ГОРИЗОНТАЛЬНОЙ ПЛОСКОЙ ПЛАСТИНОЙ

Аннотация — Аналитически исследуется линейная волновая неустойчивость ламинарного потока смешанной конвекции над изотермической горизонтальной плоской пластиной. Используемые при анализе устойчивости основные гидродинамические и тепловые поля рассматриваются как непараллельные. Система линеаризованных взаимосвязанных дифференциальных уравнений и их граничные условия для возмущений скорости и температуры составляют задачу на собственные значения, которая решается прямым методом численного интегрирования Рунге–Кутта совместно с методом итераций. Для исключения ошибок, появляющихся вследствие отбрасывания членов при численном интегрировании уравнений возмущений, используется метод фильтрации. Представлены кривые нейтральной устойчивости и критические числа Рейнольдса для диапазона значений параметра плавучести, учитывающих как попутные, так и противоположно направленные потоки при числах Прандтля 0,7 и 7. Найдено, что поток становится менее устойчивым по мере того, как подъемная сила увеличивается при попутном потоке, и более устойчивым по мере того, как подъемная сила растет при противоположно направленном потоке. Приведена диаграмма областей устойчивых и неустойчивых потоков в плоскости зависимости числа Грасгофа от числа Рейнольдса. Наконец, проведено сравнение полученных результатов по волновой неустойчивости с результатами по вихревой неустойчивости.